Author Manuscript

Author Manuscript

Author Manuscript

Author Manuscript

HHS Public Access

Author manuscript

Nanotoxicology. Author manuscript; available in PMC 2015 December 04.

Published in final edited form as:

Nanotoxicology. 2014 May ; 8(3): 317–327. doi:10.3109/17435390.2013.779757.

Effect of multi-walled carbon nanotube surface modification on bioactivity in the C57BL/6 mouse model

Tina M. Sager[1,2], **Michael W. Wolfarth**[2], **Michael Andrew**[2], **Ann Hubbs**[2], **Sherri Friend**[2], **Teh-hsun Chen**[2], **Dale W. Porter**[2], **Nianqiang Wu**[3], **Feng Yang**[4], **Raymond F. Hamilton**[1], and **Andrij Holian**[1]

[1]Department Biomedical and Pharmaceutical Sciences, University of Montana, Center for Environmental Health Sciences, Missoula, MT 59812, USA

[2]National Institute for Occupational Safety and Health, Health Effects Laboratory Division, Pathology and Physiology Research Branch, Morgantown, WV 26505, USA

[3]Department of Mechanical and Aerospace Engineering, WV Nano Initiative, West Virginia University, Morgantown, WV 26506, USA

[4]Department of Industrial and Management Systems Engineering, West Virginia University, Morgantown, WV 26506, USA

Abstract

The current study tests the hypothesis that multi-walled carbon nanotubes (MWCNT) with different surface chemistries exhibit different bioactivity profiles *in vivo*. In addition, the study examined the potential contribution of the NLRP3 inflammasome in MWCNT-induced lung pathology. Unmodified (BMWCNT) and MWCNT that were surface functionalised with -COOH (FMWCNT), were instilled into C57BL/6 mice. The mice were then examined for biomarkers of inflammation and injury, as well as examined histologically for development of pulmonary disease as a function of dose and time. Biomarkers for pulmonary inflammation included cytokines, mediators and the presence of inflammatory cells (IL-1β, IL-18, IL-33, cathepsin B and neutrophils) and markers of injury (albumin and lactate dehydrogenase). The results show that surface modification by the addition of the -COOH group to the MWCNT, significantly reduced the bioactivity and pathogenicity. The results of this study also suggest that *in vivo* pathogenicity of the BMWCNT and FMWCNT correlates with activation of the NLRP3 inflammasome in the lung.

Keywords

multi-walled carbon nanotube; surface modification; inflammasome activation; fibrosis; pulmonary toxicity

Correspondence: Tina M. Sager, National Institute for Occupational Safety and Health, 1095 Willowdale Road, M/S 2015, Morgantown, WV 26505, USA. Tel: +1 304 285 6109. Fax: +1 304 285 5938. sst2@cdc.gov.

Author Manuscript Author Manuscript Author Manuscript Author Manuscript

Introduction

Nanotechnology is emerging as one of the world's most promising new technologies. In fact, the field of nanotechnology is already a global multi-billion dollar investment market. Nanotechnology is currently at the forefront of scientific research and technological developments that have resulted in the manufacture of novel consumer products and numerous industrial applications (Musee et al. 2011). This vastly expanding area of nanotechnology offers new opportunities for making superior materials for use in industrial and biomedical applications (McAllister et al. 2002; Grassian et al. 2007). In fact, manufactured nanoparticles display physicochemical characteristics and impart unique applications within the commercial, medical and environmental sectors (Li et al. 2011a,b; Wang et al. 2010). To support the vast expansion of nanotechnology applications, a number of nanoparticles are being produced in large volumes. For example, carbon nanotubes (CNTs) are <100 nanometer diameter tubes of carbon, which are being developed and produced in mass quantities for a variety of applications. Since their discovery, many variations of CNTs have been developed, including variations in number of shells or tubes of carbon atoms. The two principal forms of CNT being utilised are the single-walled (SWCNT) and multi-walled (MWCNT) carbon nanotubes.

The applications of these CNTs include a variety of functions such as strengthening of composite materials, medical imaging, drug delivery, bone grafting, dental implants and as a key component in lithium batteries. In fact, CNTs exhibit excellent electrical, optical and chemical properties with a broad range of applications. Due to their wide range of applications, CNT production is estimated to reach into the millions of tons within the decade (Endo et al. 2008). However, even though production of CNTs are vastly increasing, the main problem with the majority of popular synthetic methods is that they produce samples yielding a mixture of various diameters and chiralities of nanotubes that are normally contaminated with metallic and amorphous impurities. Thus, functionalisation and post-synthesis chemical processing that can purify CNTs and also separate individual tubes according to diameter and chirality are proving to be viable routes to rational and predictable manipulation of the favourable electronic and mechanical properties of CNTs (Niyogi et al. 2002; Tasis et al. 2003). Therefore, a suitable functionalisation via the physical or chemical attachment of functionalities onto the CNT surface, represents a strategy for not only improving the dispersion and solubility but for also allowing strong interfacial interactions to take place between the CNT and some other entities such as polymers, biomolecules or nanoparticles (Kim 2011). In addition, functionalisation and surface modification of CNTs with organic functional molecules extends their already broad applications. Therefore, the addition of organic coatings, such as -COOH terminated coatings, alters the charge, functionality and reactivity of the CNT.

Even though CNTs offer a wide variety of applications, the development of these engineered CNTs has unfortunately surpassed evaluation of their potential human health impacts. The potential adverse health effects associated with the inhalation of airborne nanoparticles are topics of ongoing scientific and public concern (Lippman et al. 2003; Wittmaack, 2007). Due to the physical and chemical durability and fibrous nature of the CNT, concern has been raised that some of the multi-walled variety of CNTs may exhibit potentially significant

Author Manuscript Author Manuscript Author Manuscript Author Manuscript

health hazards similar to asbestos (Donaldson et al. 2006). Previous studies analysing the pulmonary toxicity of both SWCNT and MWCNT have shown that both types of CNT facilitate an increase in inflammation, fibrosis and granuloma formation (Lam et al. 2004; Shvedova et al. 2005; Porter et al. 2010; Porter et al. 2012). Therefore, previous studies have indicated that exposure to some CNTs may have adverse health impacts, which would in turn, limit or prevent the useful applications of CNT in the future. Therefore, continued evaluation of the potential toxicity of multi-walled CNTs is warranted.

One strategy that has been suggested to reduce the bioactivity of MWCNT is to alter their surface chemistry via addition of organic functional groups. Thus, in this study two different MWCNT were evaluated *in vivo*. The first had no surface modifications (i.e., as made) and was termed bare MWCNT (BMWCNT) and the second was modified by addition of carboxylic acid groups and was termed functionalised MWCNT (FMWCNT). Using these two MWCNT samples, the authors tested the hypothesis that MWCNT with different surface chemistries will exhibit different toxicity profiles *in vivo*. To test this hypothesis, mice were exposed to varying doses of BMWCNT or FMWCNT and pulmonary inflammation and pathological changes were determined. Histopathology studies to investigate the development of pulmonary disease were also conducted. In addition, to explore the hypothesis that *in vivo* inflammation and fibrosis could be facilitated by lysosomal leakage leading to inflammasome activation, the differences in bioactivity of these two MWCNT were correlated with their differential activation of the NLRP3 inflammasome.

Material and methods

Purification and functionalisation of MWCNT

Typically, 300 mg of MWCNT (Nanostructured & Amorphous Materials, Inc., Houston, TX, USA) were added into 100 ml of hydrochloric acid (HCl) (con. 36.5%), in a 250 ml three-neck flask and then sonicated for 30 min. Subsequently, the mixture was then refluxed at 80–90°C for 4 h. Next, the suspension was centrifuged after it was naturally cooled down to room temperature. The black precipitates were collected, washed with deionised water and ethanol. Finally, it was subjected to centrifugation and decantation until the pH value reached 7.0. The resulting BMWCNT were dried in a vacuum oven at room temperature overnight, and then stored in a vial for use.

FMWCNT were prepared by the oxidation of the BMWCNT in HNO_3 (con. 63%). Briefly, 300 mg of BMWCNT were added into 100 ml of HNO_3 in a three-neck flask. The mixture was then refluxed at about 110°C for 12 h. The black solution was then centrifuged to collect the FMWCNT precipitate. The FMWCNT was washed with deionised water to remove HNO_3 until a neutral solution was obtained. The resulting FMWCNT was dried in a vacuum oven at room temperature for at least 24 h.

MWCNT diameter analysis

A diameter size analysis of both the bare and functionalised MWCNT samples was conducted to demonstrate that functionalisation only affected the surfaces of MWCNT.

Author Manuscript Author Manuscript Author Manuscript Author Manuscript

Specifically, low resolution transmission electron microscopy (TEM) images were captured as described above. In order to compare the particle size distributions between the bare and the functionalised MWCNT samples, the width of a nanotube in each sample were measured using a JEOL 1220 TEM at a magnification of ×20K. Approximately 100 particles were examined from each filter sample. For the width/diameter determination, the entire size range was divided into approximately 10 successive size intervals and the number of particles (ΔN) in each interval was determined. It was necessary that the size group be contiguous and that they cover the entire size range so that no particles are left out.

Preparation of BMWCNT and FMWCNT suspensions

BMWCNT and FMWCNT were suspended in a biocompatible dispersion medium (DM) (a combination of 1,2-dipalmitoyl-sn-glycero-3-phosphocholine (DPPC) and mouse albumin in concentrations that mimic diluted alveolar lining fluid) previously described by the authors' laboratory (Porter et al. 2008). Specifically, DM is Ca^{2+}- and Mg^{2+}-free phosphate buffered saline (PBS), pH 7.4, supplemented with 5.5 mM D-glucose, 0.6 mg/ml serum albumin and 0.01 mg/ml DPPC. The DM was briefly sonicated (Branson Sonifer 450, 10W continuous output, 1 min) before use. MWCNT were then suspended in the DM to produce the desired concentration. The MWCNT suspensions were then briefly sonicated (Branson Sonifer 450, 10W continuous output, 10 min) to promote dispersion of the MWCNT samples.

Animals

C57BL/6J male mice (7 weeks old) were purchased from Jackson Laboratories (Bar Harbor, Maine, USA). Animals were housed in an AAALAC-accredited, specific pathogen-free, environmentally controlled facility and allowed to acclimate at least 7 days prior to use. The mice were monitored to be free of endogenous viral pathogens, parasites, mycoplasms, *Helicobacter* and CAR *Bacillus*. Mice were kept in ventilated cages, which were provided HEPA (high-efficiency particulate air) filtered air, with Alpha-Dri virgin cellulose chips and hardwood Beta-chips for bedding. The animals were maintained on a Harlan Teklad 7913, 6% fat, irradiated diet and tap water, both of which were provided *ad libitum*. All animal protocols were approved by the NIOSH/Morgantown Institutional Animal Care and Use Committee.

Mouse pharyngeal aspiration

Suspensions of BMWCNT and FMWCNT were prepared as described above. Mice were then exposed to 0, 2.5, 10 or 40 μg/mouse of BMWCNT or FMWCNT by pharyngeal aspiration as described by Rao et al. (2003). Briefly, the animals were anaesthetised with isoflurane and placed on a board in a near vertical position. The animal's tongue was extended with lined forceps and 50 μL of the respective particle suspension was placed on the back of the tongue, which was held until the suspension was aspirated into the lungs. Following release of the tongue, the mouse was gently lifted off the board, placed on its side and monitored for recovery from anaesthesia. Control mice were administered an equal volume of DM.

Author Manuscript Author Manuscript Author Manuscript Author Manuscript

Whole lung lavage

At 1, 7 and 56 days post-exposure, mice were weighed, a deep plane of anaesthesia was established with an intraperitoneal injection of sodium pentobarbital (>100 mg/kg), and the mice were euthanised by exsanguination. The trachea was cannulated with a blunted 22-gauge needle, and whole lung lavage (WLL) was performed using cold sterile Ca^{2+}- and Mg^{2+}-free PBS at a volume of 0.6 ml for first lavage (kept separate) and 1 ml for subsequent lavages. Approximately 4 ml WLL fluid per mouse was pooled and collected in sterile centrifuge tubes. Pooled WLL cells were washed in PBS by centrifugation (600 × *g*, 10 min, 4°C) and resuspended in PBS. First-fraction WLL aliquots with the cells removed, were frozen or kept on ice for later analysis.

Cell counts and differentials and first WLL fluid analyses

Total WLL cell counts were obtained using a Coulter Multisizer 3 (Coulter Electronics, Hialeah, FL, USA) and cytospin preparations of the WLL cells were made using a cytocentrifuge (Shandon Elliot Cytocentrifuge, London, UK). The cytospin preparations were stained with modified Wright-Giemsa stain and cell differentials were determined by light microscopy. Lactate dehydrogenase (LDH) activities and albumin concentrations of the first WWL fluid were measured to assess cytotoxicity and the integrity of the lung blood–gas barrier, respectively. LDH activities and albumin concentrations were measured using a COBAS MIRA Plus chemical analyzer (Roche Diagnostic Systems Inc., Montclair, NJ, USA) as previously described (Porter et al. 2010).

First WLL fluid assays

The presence of inflammatory mediators associated with NLRP3 activation (IL-1β, IL-18 and IL-33) in the first WLL fluid was measured 1 day post-exposure for the 40 μg/mouse dose level. The levels of the cytokines present were measured using commercially available ELISA kits (BioSource International Inc., Camarillo, CA, USA) as previously described (Hamilton et al. 2009).

To determine cathepsin B activity, the following assay components were mixed in a 96-well plate using PBS as diluent: first WLL fluid (50 μl), 2 μg Z-LR-AMC (fluorogenic Peptide Substrate, R&D systems, Minneapolis, MN, USA) ± 66 μM inhibitor (Z-Phe-Phe-FMK, MBL International, Woburn, MA, USA) in a total volume of 150 μl. The assay samples were incubated at 37°C for 1 h then fluorescence was measured using a plate reader at 380 nm excitation and 460 nm emission. Cathepsin B-specific activity was calculated as follows: relative fluorescence units (RFU) from the cathepsin B activity (no inhibitor) minus with inhibitor.

Enhanced dark field microscopy

Mice (male, C57BL/6J, 7 weeks old) were dosed with 40 μg/mouse of the specific MWCNT suspensions following the same procedures outlined above. At 56 days post-exposure, mice were euthanised by an overdose of pentobarbital (>100 mg/kg body weight, i.p.) followed by transection of the abdominal aorta to provide exsanguinations. The lungs were rapidly removed and fixed by intratracheal perfusion with 1 cc of 10% neutral buffered formalin.

Author Manuscript Author Manuscript Author Manuscript Author Manuscript

Lungs were then processed overnight in a tissue processor, and embedded in paraffin. Sections (5 μm thick) were collected on precleaned slides, deparaffinised and stained with sirius red before being cover slipped. Slides were imaged using a high signal-to-noise, dark field-based illumination on a CytoViva Olympus BX-41 microscope (CytoViva, Auburn, AL, USA) at 100× with oil immersion. Images of the lung tissue were captured with a Dage-MTI digital camera (2048 × 2048, Dage, Michigan City, IN, USA).

Histopathology

Lung histopathology was performed as previously described (Hubbs et al. 2002). Briefly, mice were anaesthetised with an intraperitoneal injection of sodium pentobarbital (>100 mg/kg) and the abdominal aorta was transected for exsanguination. Whole lungs were inflated with 1 ml of 10% neutral buffered formalin. All collected tissues were trimmed the same day, with sections of the right and left lung lobes and the tracheobronchial lymph node (TBL), if found, also trimmed. Tissues were processed overnight and embedded the following day in paraffin.

Lung sections (5 microns thick) were stained with H&E, picrosirius red and Masson's trichrome. All histology sections were interpreted by a board-certified veterinary pathologist who was blind to the experimental conditions. Microscopic evaluation included assessments of cellular uptake of the MWCNT, inflammation and fibrosis in the lung as well as particle translocation to the TBL. Each histopathologic change was scored for distribution and for severity according to the following parameters: distribution (0 = none, 1 = focal, 2 = focally extensive, 3 = multifocal, 4 = multifocal and coalescent, 5 = diffuse) and severity scores (0 = none, 1 = minimal, 2 = mild, 3 = moderate, 4 = marked, 5 = severe) as previously described by Hubbs et al. (1997). A composite score for each change consisting of the sum of the distribution and severity scores were recorded.

Statistics

Statistical comparisons between doses for each nanoparticle type (BMWCNT or FMWCNT) at a specific post-exposure time were performed separately for each post-exposure time using analysis of variance (ANOVA) with *post hoc t*-tests for pair-wise comparison of dose groups. Similar analyses were performed to compare post-exposure time effect for each nanoparticle type. Since variance estimates were different across dose groups, the ANOVA models were estimated using an unequal variance model available from SAS PROC MIXED. All statistical tests were two tailed with significance level equal to 0.05.

Since the pathology data consisted of ordinal scores rather than comparisons between control and MWCNT-exposed mice at each time, comparisons across time for each exposure group were accomplished using two separate one-way non-parametric ANOVA. Exact tests were used because of the high number of tied values in the data. The non-parametric ANOVA was performed using SAS Proc NPAR1WAY with exact Kruskal–Wallis tests for multi-group comparisons and exact Wilcoxon tests for *post hoc* pair-wise comparisons. All statistical tests were two-tailed with significance defined as type I probability of less than 5% ($p < 0.05$).

Author Manuscript Author Manuscript Author Manuscript Author Manuscript

Results

MWCNT characterisation

The samples used in this *in vivo* study were taken from the same batch employed for a companion *in vitro* study and the detailed information on the MWCNT materials utilised can be found in the authors' accompanying paper (Hamilton et al. 2012). However, a brief summary of the characterisation results is given here. The raw MWCNT received from the commercial source contained 2.2 wt% nickel (Ni) and 0.08 wt% iron (Fe). After purification treatment in HCl solution, the Ni content in the BMWCNT was reduced to 0.96 wt%, and the presence of Fe was not detected by inductively coupled plasma mass spectrometry (ICP-MS). After nitric acid (HNO_3) treatment of the BMWCNT, 0.07 wt% Ni remained in the FMWCNT and the Fe content remained lower than the limit of detection of ICP-MS. The purification treatment in HCl solution removed the amorphous carbon layer from the surface of the MWCNT sample, which was confirmed by thermogravimetric analysis (TGA). After oxidation treatment in the HNO_3 solution, the -COOH group was covalently bound to the surface of MWCNT, producing the FMWCNT. This addition of the -COOH group was confirmed by the measurement of X-ray photoelectron spectroscopy (XPS). The band at 1722 cm^{-1} in the Fourier-transform infrared (FTIR) spectrum further confirmed the presence of -COOH group. Lastly, the BMWCNT and FMWCNT samples were placed into the DM used for *in vivo* study, and the zeta potentials of each sample were obtained. The zeta potentials of BMWCNT and FMWCNT were −9.76 and −13.8 mV, respectively. The BMWCNT width had a count median diameter of 42 nm (geometric standard deviation (GSD) = 1.4). The FMWCNT width had a count median diameter of 44 nm (GSD = 1.4). Thus, the diameter analyses indicated no differences in diameter existing between the BMWCNT and FMWCNT samples. As previously mentioned, due to the fact that the CNTs are not rigid, the attempts to track single nanotubes from end to end were not successful. Therefore, it is very challenging to accurately measure the exact length of nanotubes.

Comparison of pulmonary inflammation and damage of BMWCNT and FMWCNT

At 1 day post-exposure, all doses of BMWCNT caused a significant increase in polymorphonuclear neutrophil (PMN) counts over control, while at 7 days post-exposure only the highest dose (40 μg/mouse) remained significantly elevated over the control (Figure 1A). By contrast, at 1 day post-exposure, only the highest dose (40 μg/mouse) of FMWCNT caused a significant increase in PMN versus control. This inflammatory response decreased at 7 days post-exposure, but remained significantly greater than control (Figure 1B).

Albumin levels in the first fraction of WLL fluid were analysed to assess air/blood barrier injury after MWCNT exposures. Both BMWCNT and FMWCNT caused dose-dependent increases in albumin levels. At 1 and 7 days post-exposure, all doses of BMWCNT caused a significant increase in albumin levels over control (Figure 2A). For the FMWCNT, at 1 day post-exposure, all doses caused a significant increase in albumin levels over control. However, at 7 days post-exposure, only the 40 μg/mouse dose caused a significant increase in albumin levels over control (Figure 2B).

Author Manuscript Author Manuscript Author Manuscript Author Manuscript

LDH activities were measured to assess cytotoxicity after MWCNT exposure. Similar to the PMN influx and albumin data, both BMWCNT and FMWCNT caused a dose-dependent increase in LDH activities in the WLL fluid. At 1 and 7 days post-exposure, all doses of the BMWCNT caused a significant increase in LDH activity over control (Figure 3A). For the FMWCNT, at 1 day post-exposure, all doses caused a significant increase in LDH activity over control. However, at 7 days post-exposure only the intermediate and highest doses (10 and 40 μg/mouse) of FMWCNT caused a significant increase in LDH activity over control (Figure 3B).

To compare the inflammatory response and lung pathology elicited by BMWCNT and FMWCNT, data for mice exposed to 40 μg/mouse were re-plotted for 1 and 7 days post-exposure times. These analyses indicated that relative to FMWCNT-exposed mice, BMWCNT caused substantially greater influx of PMNs, that is, 2.5- and 6.1-fold at 1 day and 7 days post-exposure, respectively (Figure 4). Relative to FMWCNT-exposed mice, BMWCNT albumin concentrations were 1.4-fold higher at 1 day post-exposure, and 2.2-fold higher at 7 days post-exposure (Figure 4B). Finally, relative to FMWCNT-exposed mice, BMWCNT LDH activities were 1.3-fold higher at 1 day post-exposure, and 1.4-fold higher at 7 days post-exposure (Figure 4C) relative to FMWCNT-exposed mice.

NLRP3 inflammasome activation

To determine if BMWCNT and FMWCNT cause phagolysosomal lysis (release of cathepsin B) and activation of the NLRP3 inflammasome, cathepsin B activities as well as IL-1β, IL-33 and IL-18 cytokine levels were measured in the first WLL fluid from mice 1 day after exposure to 40 μg/mouse doses. Cathepsin B activities for animals receiving FMWCNT and BMWCNT were significantly higher than control levels. When comparing the FMWCNT with BMWCNT, BMWCNT resulted in significantly higher (6.3-fold) levels of cathepsin B activity than FMWCNT (Figure 5A). IL-1 β levels for animals receiving FMWCNT were not significantly different than control levels of IL-1 β, but BMWCNT-exposed mice were significantly higher than controls and FMWCNT (Figure 5B). IL-18 levels of either the BMWCNT or FMWCNT exposure groups were significantly higher than control levels, with animals exposed to BMWCNT resulting in significantly higher (2-fold) levels of IL-18 than FMWCNT (Figure 5C). IL-33 levels for animals exposed to BMWCNT, but not FMWCNT, were significantly higher than control levels (Figure 5D). Taken together, the data indicate that MWCNT caused phagolysosomal lysis and activation of the NLRP3 inflammasome, which was greater in the BMWCNT compared with FMWCNT.

Enhanced dark field microscopy imaging

The enhanced dark field images taken using the CytoViva microscope at 56 days post-exposure allowed for determination of where the MWCNT are found within the lung. The results of the CytoViva microscopy studies indicate that BMWCNT are observed generally diffuse within the interstitial tissue, but also in condensed areas of alveolar macrophages (AMs) which have significant amounts of BMWCNT (Figure 6A). This outcome is drastically different for mice exposed to FMWCNT. At 56 days post-exposure, the presence of FMWCNT within the interstitial tissue is sparse, and no AMs containing FMWCNT were observable (Figure 6B). Finally, comparison of BMWCNT- and FMWCNT-exposed mice

Author Manuscript Author Manuscript Author Manuscript Author Manuscript

(Figure 6A and B) indicates that a greater amount of BMWCNT are present within the lung, suggesting BMWCNT are cleared less efficiently than the FMWCNT.

Histopathological analyses

The histopathological findings are presented in Table I. At 7 days post-exposure, the presence of phagocytosed foreign material was noted in all animals exposed to either BMWCNT or FMWCNT and was significantly different from DM-exposed vehicle controls. The severity of this finding was graded as minimal to mild, and for either MWCNT products, respectively. The degree of phagocytosis was greater in animals exposed to a dose of 40μg/mouse as compared with 2.5 μg/mouse. Occasionally, AMs that contained aggregated material formed small, several-cell clusters within alveolar lumen, which were associated with localised interstitial fibrosis. AM clusters were essentially limited to lungs that had higher distribution and severity scores for phagocytosed material. The prevalence and severity of phagocytosed foreign material were generally comparable for mice exposed to 40 μg/mouse of either BMWCNT or FMWCNT at 7 days post-exposure; however, among mice that received a 2.5 μg/mouse dose, at 7 days post-exposure, low prevalence of aggregated foreign material and foreign material within epithelial cells were only seen in mice exposed to BMWCNT.

Other histopathology findings in the lungs at 7 days post-exposure included: alveolitis (non-macrophage leucocytic infiltrates within alveolar lumina), acute bronchiolitis (primarily neutrophilic leucocytic infiltrates within bronchiolar lumina) and interstitial fibrosis (thickening of alveolar septae with increased collagen formation). The severities of these diagnoses were uniformly minimal, and their prevalence tended to be only slightly higher in treated mice versus untreated controls. At the 40 μg/mouse dose, alveolitis and fibrosis for BMWCNT tended to exceed that for FMWCNT, consistent with the WLL inflammatory biomarkers.

TBL: 7 days post-exposure

The only clear treatment-related finding in the TBL was the presence of phagocytosed foreign material, which occurred in animals exposed to either BMWCNT or FMWCNT. The foreign material, which was virtually identical to foreign material in the lung, was present within the cytoplasm of macrophages that were scattered primarily throughout the paracortex and medulla. The severity of this finding was minimal in all affected TBL.

Lung: 56 days post-exposure

At 56 days post-exposure, the presence of phagocytised foreign material appeared qualitatively similar to the material observed at 7 days post-exposure. The prevalence of phagocytosed foreign material (including material within alveolar epithelial cells) in both types of BMWCNT and FMWCNT at both dose concentrations (2.5 and 40 μg/mouse) tended to be slightly lower in day 56 animals as compared with mice of the day 7 sacrifice.

Also, at 56 days post-exposure, interstitial fibrosis was observed nearly exclusively in mice treated with 40 μg/mouse of BMWCNT (Figure 7), and there was a moderate prevalence of alveolitis that was limited entirely to mice exposed to BMWCNT at 40 μg/mouse (Table I).

Author Manuscript Author Manuscript Author Manuscript Author Manuscript

The prevalence of alveolitis and interstitial fibrosis in mice exposed to 40 μg/mouse BMWCNT was significantly greater than the prevalence in control or FMWCNT mice (Table I). These fibrosis data are consistent with and supported by the CytoViva dark field image analyses showing that the BMWCNT are more persistent than the FMWCNT within the interstitial tissue of the lung at 56 days post-exposure.

TBL: 56 days post-exposure

In mice sacrificed on day 56, the sole treatment-related finding in the TBL was the presence of phagocytosed foreign material, which occurred in animals exposed to 40 μg/mouse of either BMWCNT or FMWCNT (Table I). Mean severity scores for this finding were slightly higher for day 56 mice as compared with day 7 mice. Similar to day 7 mice, the generally low prevalence and severity of haemosiderin-laden macrophages in TBL subscapular sinuses of day 56 mice were comparable among control and treated animals.

Discussion

Over the last 20 years, CNT have received considerable attention from many researchers due to their interesting properties and broad applications. In addition to their outstanding mechanical characteristics, CNT exhibit excellent electrical and thermal properties. These superior properties provide exciting opportunities to produce advanced materials for new applications (Dresselhaus et al. 2001; Abuilaiwi et al. 2010). Because of the rapid growth in the manufacturing and use of CNT, concerns have been raised about their potential adverse effects on both human health and the environment. The present study specifically examined the potential pulmonary responses to MWCNT exposure and the effects of surface modification of the MWCNT, in particular the addition of carboxyl groups, to assess if surface carboxylation reduces the bioactivity of the nanomaterial *in vivo*. Mechanistically, the current study also evaluated if the *in vivo* bioactivity of MWCNT correlates with activation of the NLRP3 inflammasome (Figure 8).

Effect of surface modification on the bioactivity of MWCNT

Surface modification of MWCNT with functional moieties is a key step to extend their applications in biological and industrial areas. The surface functional groups can alter the surface charge and reactivity of the surface, and enhance the stability and dispersion of MWCNT. For example, functionalisation of MWCNT with the COOH moiety can change the MWCNT from a hydrophobic state to hydrophilic state, thus providing active sites for further conjugation. Furthermore, carboxylation of MWCNT can result in a less hydrophobic, more negatively charged particle, which may affect how cells interact with the MWCNT.

Therefore, the first hypothesis of this study was that surface modification, in particular the addition of carboxylic acid groups to the MWCNT surface, would reduce their bioactivity *in vivo* in a similar manner to what we observed *in vitro* (Hamilton et al. 2012). The current study results show that this surface modification did significantly reduce the bioactivity of the MWCNT. In fact, the inflammatory response elicited by the FMWCNT was approximately 2.5- and 6.1- fold lower than the BMWCNT response at both 1 and 7 days

Author Manuscript Author Manuscript Author Manuscript Author Manuscript

post-exposure, respectively. The air–blood barrier injury induced by exposure to the BMWCNT (40 μg/mouse) was 1.4- and 2.2-fold greater than FMWCNT at 1 and 7 days post-exposure, respectively. LDH activity in lung lavage fluid elicited by the highest dose of the BMWCNT was 1.3- and 1.4-fold greater at 1 and 7 days post-exposure, respectively. These results indicate that modifying the surface of the MWCNT with the -COOH group did in fact lower the bioactivity of the MWCNT.

As previously mentioned, the addition of surface functional groups can enhance the dispersion of the MWCNT. Previous studies have reported that well-dispersed MWCNT were found to be more bioactive in the lung, causing more inflammation and fibrosis than the same dose of poorly dispersed MWCNT (Wang et al. 2010; Shvedova et al. 2008). Furthermore, in studies utilising spherical metal oxide nanoparticles, the authors have previously shown that the more dispersed the nanoparticle solution administered *in vivo* or *in vitro*, the greater degree of bioactivity of the nanoparticles (Sager et al. 2007; Sager et al. 2008). These past studies established dispersion status as a critical factor in determining MWCNT and spherical nanoparticle bioactivity and fibrogenicity. However, in the current study, surface modification, not CNT dispersion status of the MWCNT was the primary driving force behind differential bioactivity and fibrogenicity in the lung. In order to focus on the effects of surface functionalisation, the current study was able to eliminate the variable of dispersion status by producing well-dispersed MWCNT samples. The results of the study shows that a well-dispersed FMWCNT is less bioactive in the lung, causing significantly less inflammation and fibrosis when compared with the same unmodified well-dispersed BMWCNT. These results therefore indicate that surface modification with functionalisation promotes the “safety by design” concept in regards to MWCNT production and utilisation.

The results of the current study are consistent with the findings of other studies investigating the pulmonary toxicity of MWCNT. For example, Tabet et al. (2011) reported that coating MWCNT with polystyrene significantly lowered the pulmonary cytotoxicity and inflammation when compared with the untreated MWCNT. A study conducted by Kim et al. (2010) reported that the unmodified MWCNT caused significantly more inflammation in the lung than acid-treated MWCNT. Another recent study conducted by Wang et al. (2012) reported that MWCNT suspended in pluronic F108 possessed a higher degree of dispersion than the MWCNT suspended in bovine serum albumin (BSA). However, exposures to MWCNT suspended in the BSA were more fibrogenic and *in vivo* than exposures to the same concentration of pluronic F108 suspended MWCNT. The Wang *et al*. study concluded that pluronic F108 coated the MWCNT in a manner that they were unable to facilitate cellular events (e.g., phagolysosomal disruption) necessary to induce pathogenesis of pulmonary fibrosis. Taken together, these results demonstrate that coating the MWCNT surface with substances such polystyrene or pluronic F108 or functionalising the MWCNT surface, without affecting their intrinsic structure, may constitute a useful strategy for decreasing MWCNT toxicity. However, it is highly probable that the effect of coating or functionalising the surface of MWCNT on toxicological outcomes will be dependent on coating and/or functional group specific. Therefore, the degree to which a specific coating or

Author Manuscript Author Manuscript Author Manuscript Author Manuscript

functional group may decrease MWCNT toxicity should be assessed on a case-by-case basis.

Role of the NLRP3 inflammasome activation on MWCNT bioactivity

Based on the findings discussed above, the overall conclusion of the current study was that BMWCNT were more bioactive than the FMWCNT. Thus, the authors wanted to further investigate the basis for this difference in bioactivity. Previous data from the authors' laboratory have shown that titanium dioxide (TiO_2) nanobelts were highly toxic to AMs *in vitro*, but TiO_2 nanospheres were not (Hamilton et al. 2009). This study also provided evidence that this differential toxicity was related to activation of the NLRP3 inflammasome. Furthermore, an *in vivo* study conducted by Yazdi et al. (2010) concluded that mice subjected to inhalation exposure of nano-TiO_2 developed lung inflammation catalysed by the activation of the NLRP3 inflammasome, leading to IL-1β release. To support their conclusion of the NLRP3 inflammasome-induced inflammatory response, Yazdi *et al*. showed that the inflammatory response to the same nano-TiO_2 exposure was decreased in IL-1β deficient mice. Thus, these findings propelled us to investigate if the mechanism responsible for the difference in bioactivity of BMWCT versus FMWCNT might also be differential activation of the NLRP3 inflammasome.

Current evidence suggests that toxic nanoparticles could potentially increase phagolysosomal membrane permeability and release of cathepsin B causing activation of the NLRP3 inflammasome, which induces the release of pro-inflammatory cytokines (IL-1β and IL-18) from AMs and most likely IL-33 from epithelial cells (Figure 8) (Beamer et al. 2012). This family of cytokines has been shown to significantly contribute to the acute inflammatory response, for example, PMN infiltration (Hamilton et al. 2009) as well as fibrosis (Wang et al. 2012) both *in vitro* and *in vivo*. In fact, a recent study by Beamer et al. (2012) has shown that MWCNT exposure in C57BL/6 mice resulted in elevated levels of IL-33 in the lavage fluid. The findings of Beamer et al. (2012) also support the findings of the current study, which suggests that activation of the NLRP3 inflammasome induces the release of IL-33 from epithelial cells as a result of MWCNT exposure, in turn promoting the acute inflammatory response.

When inhaled particles, including MWCNT, deposit in the distal airways and alveoli, they are engulfed by AMs. AMs are present in the alveoli and on the surface of distal airways, and these pneumocytes are capable of phagocytising particles (Bals et al. 1999). During the phagocytosis process, the MWCNT are taken up into the macrophage's phagolysosomes. This uptake into the phagolysosome of specific bioactive particles catalyses damage, phagolysosome leakage and cathepsin B release. This initial release of cathepsin B initiates the activation of the NLRP3 inflammasome, which cleaves the inactive pro forms of IL-1β, IL-18 and IL-33 to active forms of these cytokines. These cytokines are secreted into the alveolar lining fluid of the lung and in turn synergistically work to promote inflammation and fibrosis in the lung (Cassel et al. 2009).

In the present study, cathepsin B activity and IL-1β, IL-18 and IL-33 levels in the WLL fluid were monitored 1 day after exposure to 40 μg/mouse of BWMCT and FMWCNT. The results of the current study support the NLRP3 inflammasome activation hypothesis.

Author Manuscript Author Manuscript Author Manuscript Author Manuscript

Specifically, cathepsin B activities for animals receiving BMWCNT and FMWCNT were significantly higher than control levels. However, when comparing BMWCNT with FMWCNT, the BMWCT caused significantly higher (6.3-fold greater) levels of cathepsin B activity than FMWCNT. Furthermore, the BMWCNT-exposed mice had significantly higher levels of IL-1β, IL-18 and IL-33 than FMWCNT. These findings are consistent with results from the *in vitro* studies (Hamilton et al. 2012) supporting the notion that *in vitro* studies of NLRP3 inflammasome activation could be used to predict *in vivo* outcomes.

Therefore, it is evident from the findings of the current study that NLRP3 inflammasome activation is potentially the driving force behind both the inflammatory and fibrogenic response of MWCNT exposure. However, it is important to note that functionalisation of the MWCNT surface downregulates activation of the NLRP3 pathway, significantly lessening the degree of inflammation and fibrosis in response to MWCNT exposure. More specifically, when comparing bare-unmodified MWCNT (BMWCNT) to surface modified (FMWCNT), it was found that the BMWCNT were pathogenically more bioactive in the lung, causing a more robust inflammatory and fibrotic response than FMWCNT. Not only did the BMWCNT cause a more acute pulmonary response in the lung (as indicated by PMN influx and greater LDH activity and albumin levels in BAL samples), the BMWCNT were also more fibrotic at 56 days post-exposure.

In conclusion, this current study suggests that the NLRP3 inflammasome is activated *in vivo*, after pulmonary exposure to MWCNT, and the extent of the activation was decreased by addition of -COOH on the surface of BMWCNT. The findings support the notion that the NLRP3 inflammasome plays a crucial role in the pathogenic response to MWCNT. In fact, data from the present study support a relationship between the extent of NLRP3 inflammasome activation by BMWCNT or FMWCNT and the degree of pulmonary inflammation and fibrosis.

The results confirm that modification of the surface chemistry of the MWCNT with COOH-groups decreased their bioactivity. Specifically, the BMWCNT were more bioactive, causing more inflammation, lung pathology and fibrosis than the FMWCNT. This difference in bioactivity also correlated with the activation of the NLRP3 inflammasome. Furthermore, evidence provided from this study indicates that activation of the NLRP3 inflammasome is a good predictor of lung pathogenesis. In conjunction with the findings of the current study, many recent therapeutic goals to treat chronic inflammation in the lung have focused on interrupting or blocking the NLRP3 inflammasome pathway (Arend et al. 2008). It would be interesting to determine if this relationship holds true for other classes of engineered nanoparticles as well. These results certainly hold promise for “safety by design” efforts to improve occupational and environmental safety.

The present study is a part of a larger program with the goal of establishing what physicochemical properties of nanomaterials influence their pathogenicity. In turn, identifying important physicochemical properties contributing to nanoparticle pathogenicity could lead to the development of predictive model(s) of nanoparticle bioactivity. In the future, such information may allow material scientists to incorporate a “safety by design”

Author Manuscript Author Manuscript Author Manuscript Author Manuscript

philosophy into the development of new nanoparticle-based technologies, which will use nanomaterials that pose lower risks to human health.

Acknowledgements

Figure 8 of this manuscript was drafted by Mr. Kevin Trout at the University of Montana, Center for Environmental Health Sciences, Department Biomedical and Pharmaceutical Sciences.

Declaration of interest

The work discussed in this manuscript was supported in part by grant RC2 ES-018742 and NSF grant CBET-0834233. The production and characterisation work was financially supported by a NIH grant (1RC2ES018742-01). The facilities and resources used in this work were partially supported by the NSF grant (EPS 1003907) with matching funds from the West Virginia University Research Corporation and the West Virginia EPSCoR Office. The findings and conclusions in this report are those of the authors and do not necessarily represent the views of the National Institute for Occupational Safety and Health.

References

Abuilaiwi F, Laoui T, Al-Harthi M, Atieh MA. Modification and functionalization of multiwalled carbon nanotube (MWCNT) via Fischer esterification. Arabian J Sci Eng. 2010; 35 Number 1C.

Arend W, Palmer G, Gagay C. IL-1, IL-18, and IL-33 families of cytokines. Immunol Rev. 2008; 223:20–38. [PubMed: 18613828]

Bals R, Weiner D, Wilson J. The innate immune system in cystic fibrosis lung disease. J Clin Invest. 1999; 103:303–307. [PubMed: 9927489]

Beamer CA, Girtsman TA, Seaver BP, Finsaas KJ, Migliaccio CT, Perry VK, et al. IL-33 mediates mutli-walled carbon nanotube (MWCNT)-induced airway hyper-reactivity via the mobilization of innate helper cells in the lung. Nanotoxicology. 2012 Epub ahead of print, June 29.

Brozena AH, Moskowitz J, Shao B, Deng S, Liao H, Gaskell KJ, et al. Outer wall selectively oxidized, water-soluble double-walled carbon nanotubes. J Am Chem Soc. 2010; 132:3932–3938. [PubMed: 20178323]

Cassel S, Eisenbarth S, Iyer S, Sadler J, Colegio O, Tephly L, et al. The Nalp3 inflammasome: a sensor of immune danger signals. Semin Immunol. 2009; 21:194–198. [PubMed: 19501527]

Datsyuk V, Kalyva M, Papagelis K, Parthenios J, Tasis D, Siokou A, et al. Chemical oxidation of multiwalled carbon nanotubes. Carbon. 2008; 46:833–840.

Donaldson K, Aitken R, Tran L, Stone V, Duffin R, Forrest G, et al. Carbon nanotubes: a review of their properties in relation to pulmonary toxicology and workplace safety. Toxicol Sci. 2006; 92(1): 5–22. [PubMed: 16484287]

Dresselhaus, M.; Dresselhaus, G.; Avouris, P. Carbon nanotubes: synthesis, structure, properties, and applications. Germany: Springer-Verlag Berlin Heidleberg: 2001.

Endo M, Strano M, Ajayan P. Carbon Nanotubes: potential applications of carbon nanotubes. Top Appl Phys. 2008; 111:13–61.

Grassian V, O'Shaughnessy P, Adamcakova-Dodd A, Pettibone J. Inhalation exposure study of titanium dioxide nanoparticles with a primary particle size of 2 to 5 nm. Environ Health Perspect. 2007; 115(3):397–402. [PubMed: 17431489]

Hamilton R Jr, Wu N, Porter D, Buford M, Wolfarth M, Holian A. Particle length-dependent titanium dioxide nanomaterials' toxicity and bioactivity. Particle Fibre Toxicol. 2009; 6:35–41.

Hamilton R Jr, Xiang C, Li M, Ka I, Yang F, Ma D, et al. Purification and sidewall functionalization of multi-walled carbon nanotubes and resulting bioactivity in macrophages from C57Bl/6 Mice. Toxicology. 2012 Submitted to Inhal.

Hubbs A, Battelli L, Goldsmith W, Porter D, Frazer D, Friend S, et al. Necrosis of nasal and airway epithelium in rats inhaling vapors of artificial butter flavoring. Toxicol Appl Pharmacol. 2002; 185:128–135. [PubMed: 12490137]

Author Manuscript Author Manuscript Author Manuscript Author Manuscript

Hubbs AF, Castanova V, Ma JYC, Frazer DG, Siegel PD, Ducatman BS, et al. Acute lung injury induced by a commercial leather conditioner. Toxicol Appl Pharmacol. 1997; 143:37–46. [PubMed: 9073590]

Kim, J. Functionalization of carbon nanotubes: In carbon nanotubes for polymer reinforcement. Boca Raton, FL: CRC Press, Taylor and Francis Group Publishing; 2011. p. 69-114.

Kim J, Lim H, Miani-Tehrani A, Kwon J, Shin J, Woo C, et al. Toxicity and clearance of intratracheally administered multiwalled carbon nanotubes from murine lung. J Toxicol Environ Health. 2010; 73:1530–1543.

Lam C-W, James JT, McCluskey R, Hunter RL. Pulmonary toxicity of single-wall carbon nanotubes in mice 7 and 90 days after intratracheal instillation. Toxicol Sci. 2004; 77(1):126–134. [PubMed: 14514958]

Li M, Li R, Li C, Wu N. Electrochemcial and optical biosensors based on nanomaterials and nanostructures: review. Front Biosci. 2011a; S3:1308–1331.

Li M, Cushing S, Wang Q, Shi X, Hownak L, Hong Z, et al. Size-dependent energy transfer between CdSe/ZnS quantum dots and gold nanoparticles. J Phys Chem Lett. 2011b; 2:2125–2129.

Lippman M, Frampton M, Schwartz J, Dockery D, Schlesinger R, Koutrakis P. The U.S. Environmental Protection Agency particulate matter health effects research centers program: a midcourse report of status, progress, and plans. Environ Health Perspect. 2003; 111:1074–1092. [PubMed: 12826479]

Long T, Tilton R, Lowry G, Veronesi B. Titanium dioxide (P25) produces reactive oxygen species in immortalized brain microglia (BV2): implications for nanoparticle neurotoxicity. Environ Sci Technol. 2006; 40(14):4346–4352. [PubMed: 16903269]

McAllister K, Sazani P, Adam M, Cho M, Rubinstein M, Samuluski R. Polymeric nanogels produced via inverse micro-emulsion polymerization as potential gene and antisense delivery agents. J Am Chem Soc. 2002; 124:15198–15207. [PubMed: 12487595]

Muller J, Huaux F, Moreau N, Mission P, Heilier JF, Delos M, et al. Respiratory toxicity of multi-wall carbon nanotubes. Toxicol Appl Pharmacol. 2005; 207:221–231. [PubMed: 16129115]

Musee N, Thwala M, Nota N. The antibacterial effects of engineered nanomaterials: implications for wastewater treatment plants. J Environ Monit. 2011; 13(5):1164–1170. [PubMed: 21505709]

Niyogi S, Hamon M, Hu H, Zhao B, Bhowmik P, Sen R, et al. Chemistry of Single-Walled Carbon Nanotubes. Acc Chem Res. 2002; 35(12):1105–1113. [PubMed: 12484799]

Porter D, Barger M, Robinson V, Leonard S, Landsittel D, Castranova V. Comparison of low doses of aged and freshly fractured silica on pulmonary inflammation and damage in the rat. Toxicology. 2002; 175:63–71. [PubMed: 12049836]

Porter D, Hubb A, Chen T, McKinney W, Mercer R, Wolfarth M, et al. Acute pulmonary dose-responses to inhaled multi-walled carbon nanotubes. Nanotoxicology. 2012 Epub ahead of print.

Porter D, Sriram K, Wolfarth M, Jefferson A, Schwegler-Berry D, Andrew M, et al. A biocompatible medium for nanoparticle dispersion. Nanotoxicology. 2008; 2:144–154.

Porter DW, Hubbs A, Mercer R, Wu N, Wolfarth M, Sriram K, et al. Mouse pulmonary dose and time course-responses induced by exposure to multi-walled carbon-nanotubes. Toxicology. 2010; 269:136–147. [PubMed: 19857541]

Pumera M. Carbon nanotubes contain residual metal catalyst nanoparticles even after washing with nitric acid at elevated temperature because these metal nanoparticles are sheathed by several graphene sheets. Langmuir. 2007; 23:6453–6458. [PubMed: 17455966]

Ramanathan T, Fisher FT, Ruoff RS, Brinson LC. Amino-Functionalized Carbon Nanotubes for Binding to Polymers and Biological Systems. Chem Mater. 2005; 17:1290–1295.

Rao G, Tinkle S, Weissman D, Antonini J, Kashon M, Salmen R, et al. Efficacy of a technique for exposing the mouse lung to particles aspirated from the pharynx. J Toxicol Environ Health Part A. 2003; 66:1441–1452. [PubMed: 12857634]

Sager T, Porter T, Robinson V, Lindsley W, Schwegler-Berry D, Castranova V. Pulmonary response to intratracheal instillation of ultrafine versus fine titanium dioxide: role of particle surface area. Particle and Fibre Toxicology. 2008; 5:17. [PubMed: 19046442]

Sager TM, Kommineni C, Castranova V. The Improved method to disperse nanoparticles for in vitro and in vivo investigation of toxicity. Nanotoxicology. 2007; 1(2):118–129.

Author Manuscript Author Manuscript Author Manuscript Author Manuscript

Shvedova A, Kisin R, Mercer R, Murray R, Johnson V, Potapovich A, et al. Unusual inflammatory and fibrogenic pulmonary responses to single-walled carbon nanotubes in mice. Lung Cell Mole Physiol. 2005; 289:L698–L708.

Shvedova A, Kisin E, Murray R, Johnson V, Gorelik O, Arepalli S, et al. Inhalation vs. aspiration of single-walled carbon nanotubes in C57BL/6 mice: inflammation, fibrosis, oxidative stress, and mutagenesis. Lung Cell Mole Physiol. 2008; 295(4):L552–L565.

Tabet L, Bussy C, Setyan A, Deckers A, Rossi M, Boczkowski J, et al. Coating carbon nanotubes with polystyrene-based polymer protects against pulmonary toxicity. Part Fibre Toxicol. 2011; 8:3-1-13. [PubMed: 21255417]

Tasis D, Tagmatarchis N, Georgakilas V, Prato M. Soluble carbon nanotubes. Chem Eur J. 2003; 9(17):4000–4008. [PubMed: 12953186]

Wang D, Zhao H, Wu N, El Khakani A, Ma D. Tuning the charge transfer property of PbS-quantum dot/TiO2-nanobelt nanohybrids via quantum confinement. J Phys Chem Lett. 2010; 1:1030–1035.

Wang X, Xia T, Duch M, Ji Z, Zhang H, Li R, et al. Pluronic F108 coating decreases the lung fibrosis potential of multiwall carbon nanotubes by reducing lysosomal injury. Nano Lett. 2012; 12:3050–3061. [PubMed: 22546002]

Wittmaack K. In search of the most relevant parameter for quantifying lung inflammatory response to nanoparticle exposure: particle number, surface area, or what? Environ Health Perspect. 2007; 115(2):187–194. [PubMed: 17384763]

Wu NQ, Fu L, Su M, Aslam M, Wong KC, Dravid VP. Interaction of fatty acid monolayers with cobalt nanoparticles. Nano Lett. 2004; 4:383–338.

Yazdi A, Guarda G, Riteau N, Drexler S, Tardivel A, Couillin I, et al. Nanoparticles activate the NLR pyrin domain containing 3 (Nlrp3) inflammasome and cause pulmonary inflammation through release of IL-1α and IL-1β. Proc Natl Acad Sci. 2010; 107(45):19449–19454. [PubMed: 20974980]

Author Manuscript Author Manuscript Author Manuscript Author Manuscript

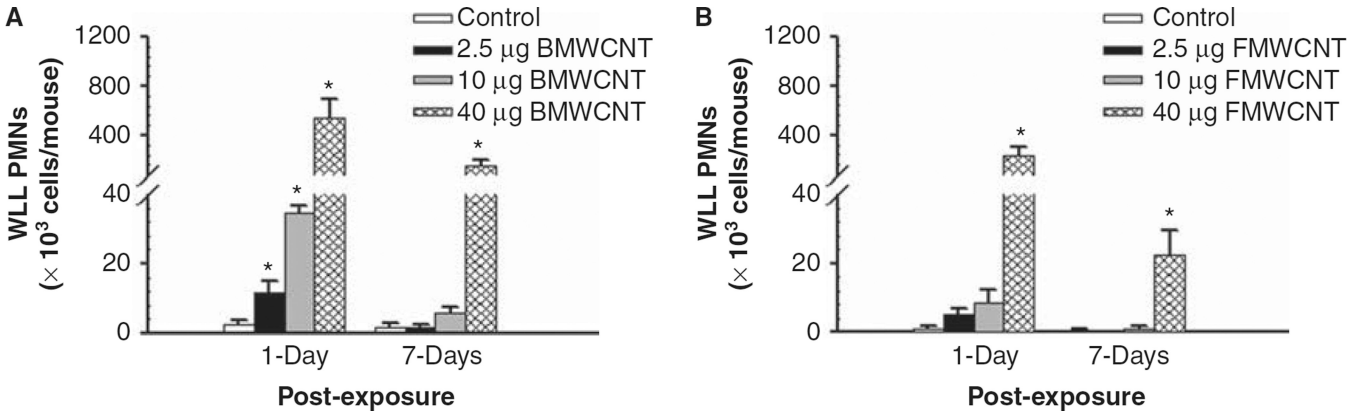

Figure 1.

Comparison of inflammation induced by pharyngeal aspiration exposure to 0, 2.5, 10 and 40 μg/mouse of BMWCNT (A) and FMWCNT (B) at 1 and 7 days post-exposure. WLL PMNs were used as a marker of pulmonary inflammation. Values are given as means ± SE (n = 8). An asterisk (*) indicates that PMN influx for that group were significantly higher than control ($p < 0.05$).

Author Manuscript

Author Manuscript

Author Manuscript

Author Manuscript

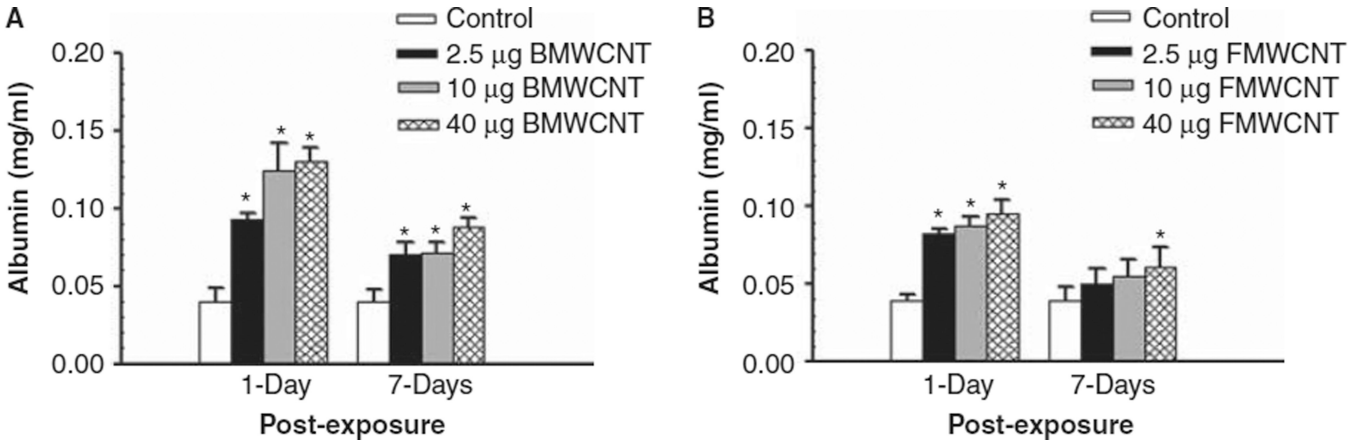

Figure 2.

Comparison of air/blood barrier injury induced by pharyngeal aspiration exposure to 0, 2.5, 10 and 40 μg/mouse of BMWCNT (A) or FMWCNT (B) at 1 and 7 days post-exposure. WLL fluid albumin concentrations were used as a marker of the air/blood barrier. Values are given as means ± SE (n = 8). An asterisk (*) indicates that albumin levels for that group were significantly higher than control ($p < 0.05$).

Author Manuscript Author Manuscript Author Manuscript Author Manuscript

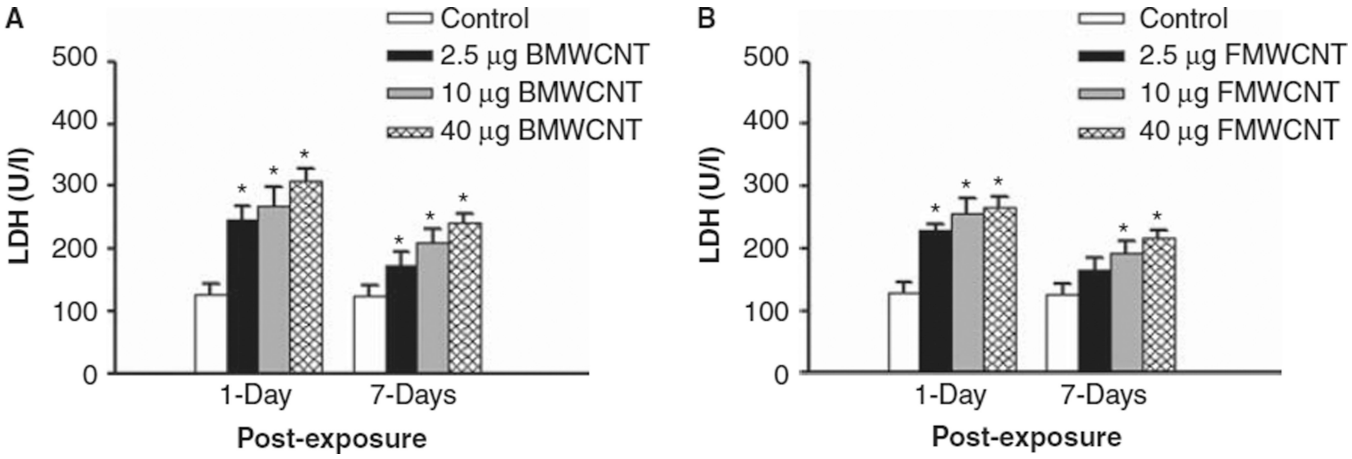

Figure 3.

Comparison of cytotoxicity induced by pharyngeal aspiration exposure to 0, 2.5, 10 and 40 μg/mouse of BMWCNT (A) or FMWCNT (B) at 1 and 7 days post-exposure. WLL fluid LDH activities were used as a marker of cytotoxicity. Values are given as means ± SE (n = 8). An asterisk (*) indicates that LDH activity for that group was significantly higher than control ($p < 0.05$).

Author Manuscript Author Manuscript Author Manuscript Author Manuscript

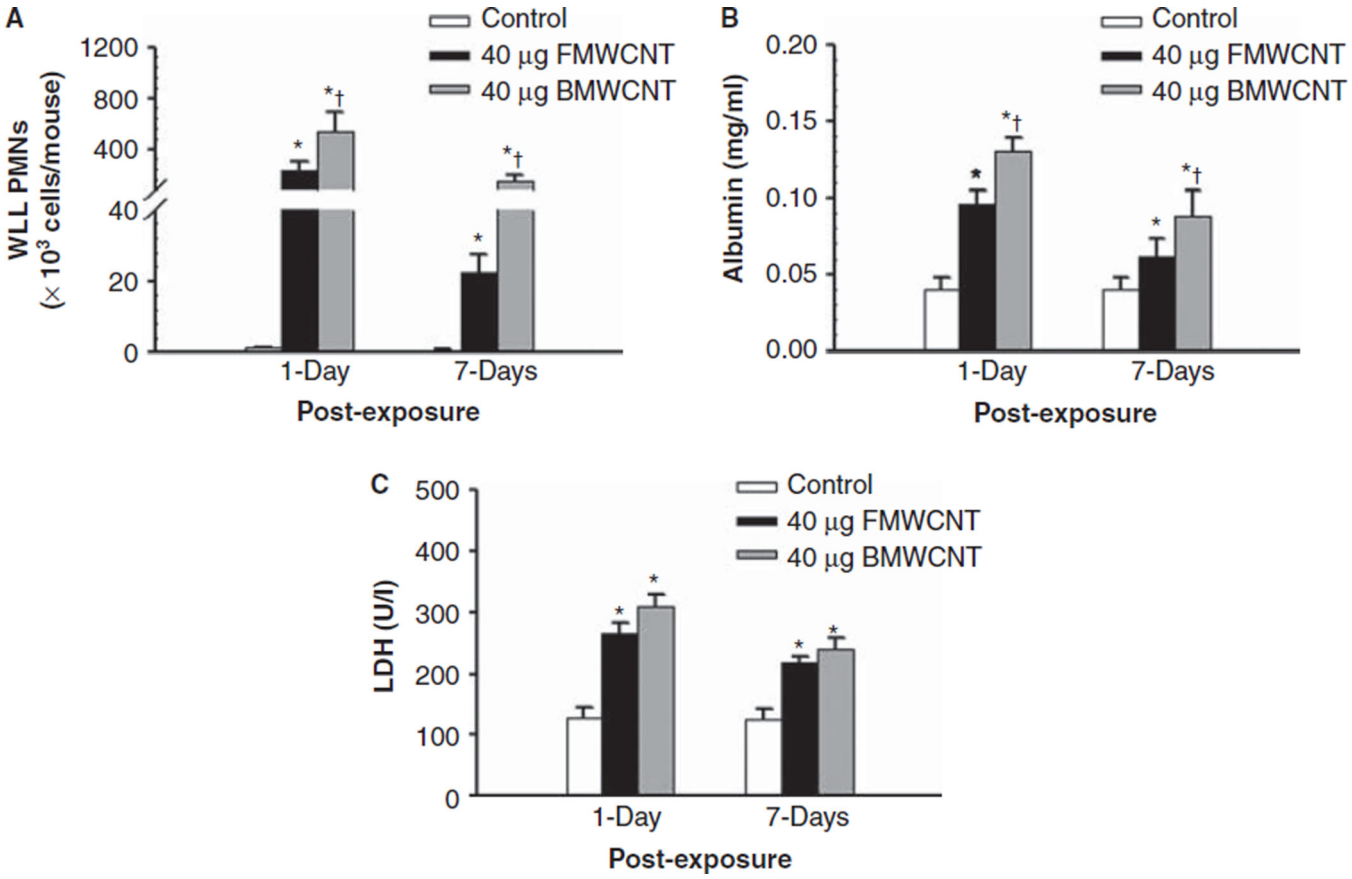

Figure 4.

Comparison of inflammation (A), air/blood barrier injury (B) and cytotoxicity (C) induced by pharyngeal aspiration exposure to 40 µg/mouse of BMWCNT or FMWCNT at 1 and 7 days post-exposure. Values are given as means ± SE (n = 8). An asterisk (*) indicates that levels for that group were significantly higher than control ($p < 0.05$). A (+) indicates that BMWCNT elicited levels that were significantly higher than FMWCNT ($p < 0.05$).

Author Manuscript Author Manuscript Author Manuscript Author Manuscript

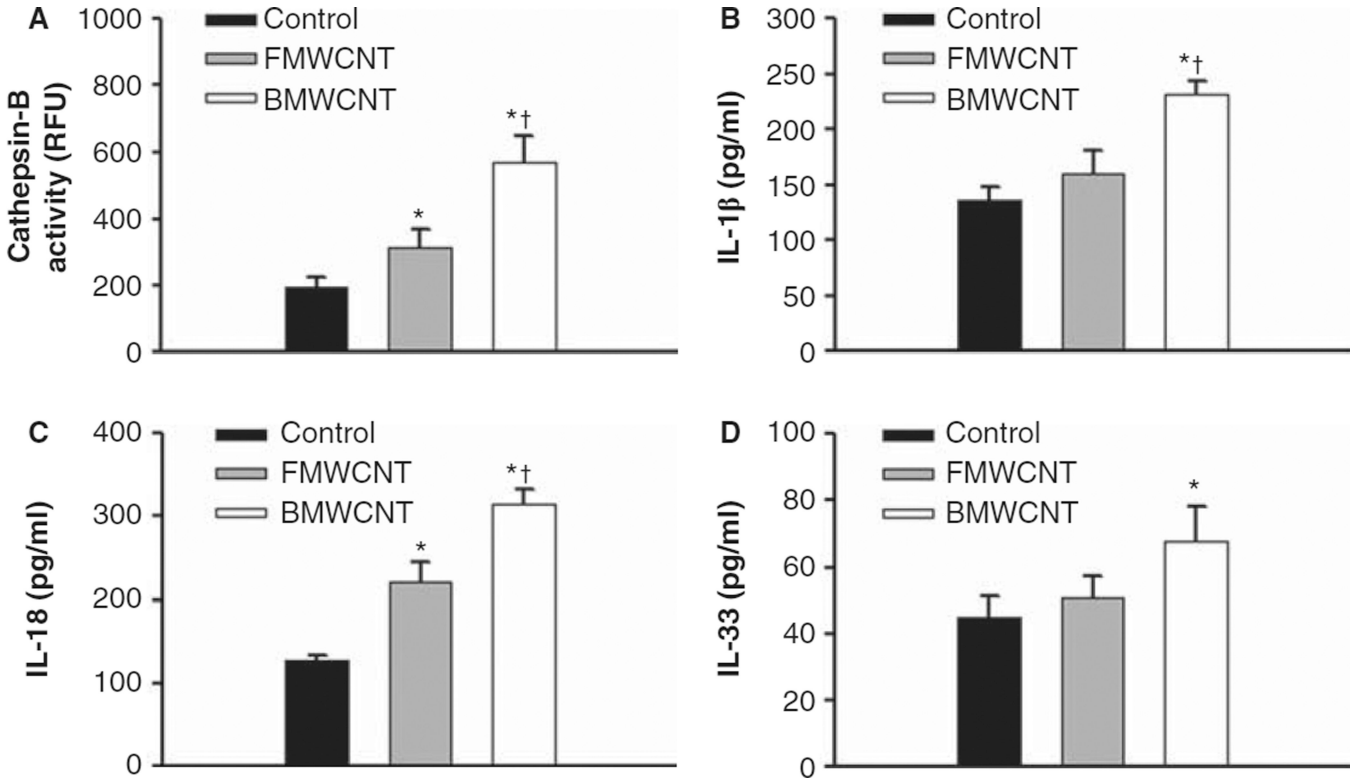

Figure 5.

Differential activation of the NLRP3 inflammasome by BMWCNT and FMWCNT. Mice were exposed by pharyngeal aspiration to 0 or 40 μg/mouse of either BMWCNT or FMWCNT and first WLL fluid was isolated at 1 day post-exposure. Cathepsin B activities (A) and concentrations of IL-1β (B), IL-18 (C) and IL-33 (D) were determined as described in the section "Materials and Methods". Values are means ± SE ($n = 8$). An asterisk (*) indicates significant increase vs. control ($p < 0.05$). A (+) indicates that BMWCNT was significantly greater than FMWCNT ($p < 0.05$).

Author Manuscript Author Manuscript Author Manuscript Author Manuscript

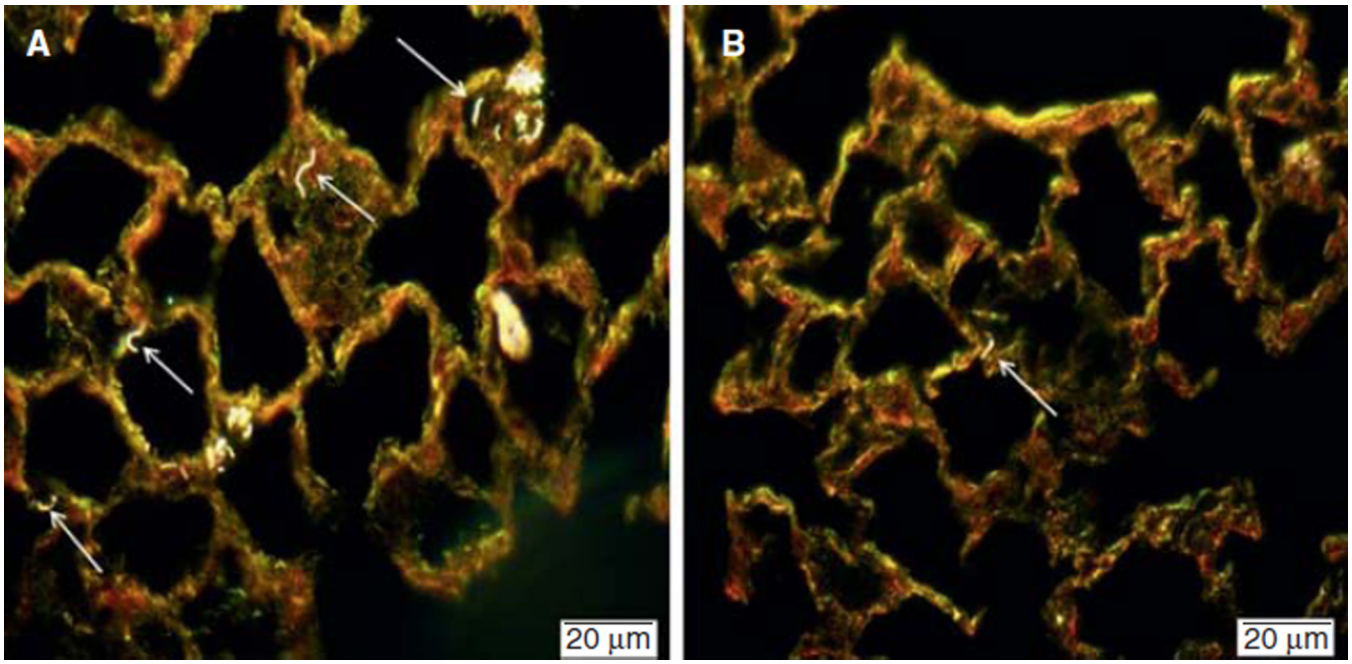

Figure 6.
Enhanced dark field imaging of BMWCNT (A) and FMWCNT (B) in mouse lungs at 56 days post-exposure. Arrows indicate presence of MWCNT.

Author Manuscript Author Manuscript Author Manuscript Author Manuscript

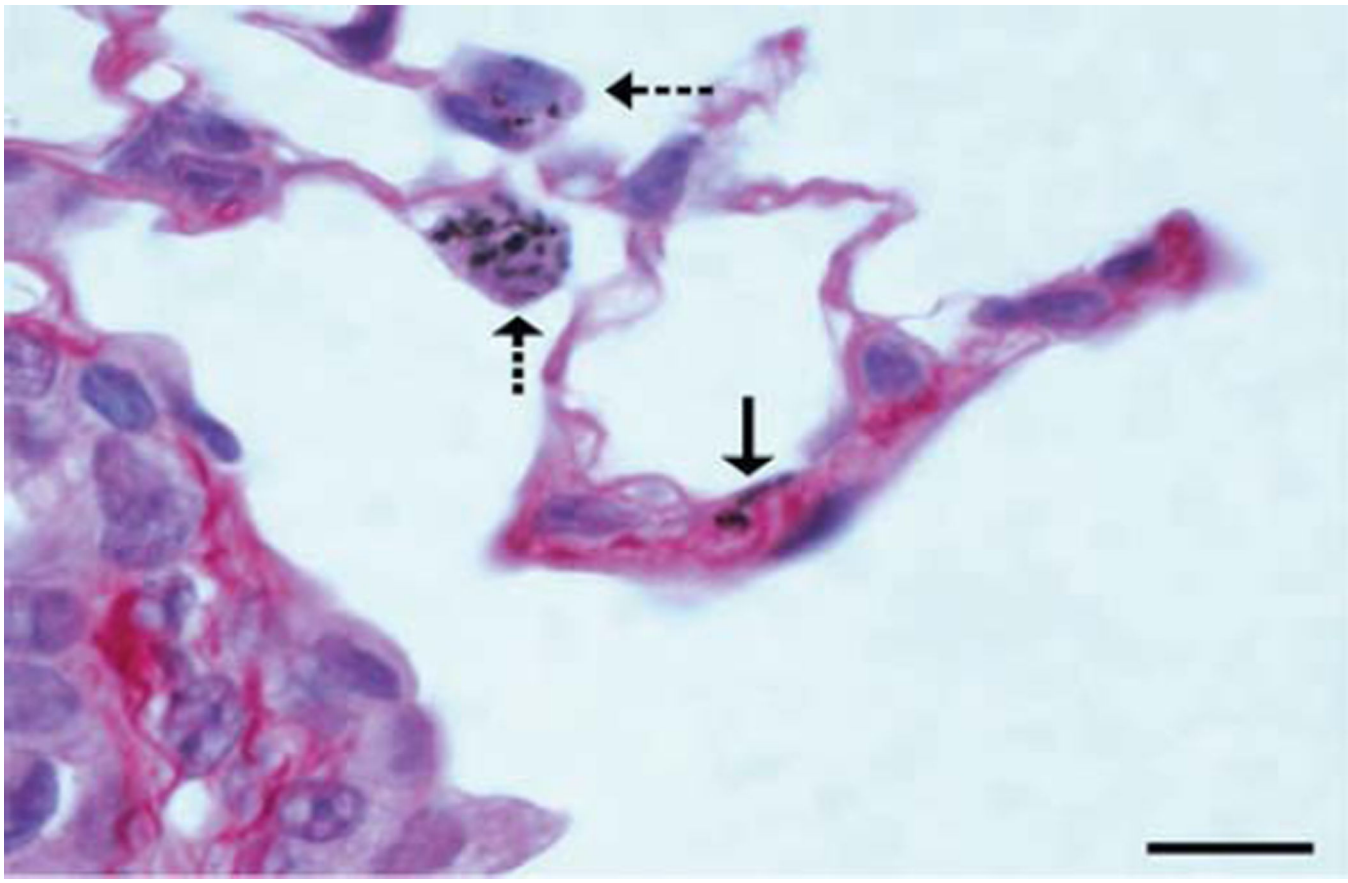

Figure 7.

Photomicrograph from the lung of a mouse 56 days after a single aspiration exposure to BMWCNT. Mild alveolar septal fibrosis is in the wall of an alveolar duct and is associated with interstitial BMWCNT (solid arrow). Macrophages contain phagocytised BMWCNT (dashed arrows). The nucleus in one of the macrophages is undergoing karyolysis, which suggests cytotoxicity. Sirius red stain; bar = 10 μm.

Author Manuscript Author Manuscript Author Manuscript Author Manuscript

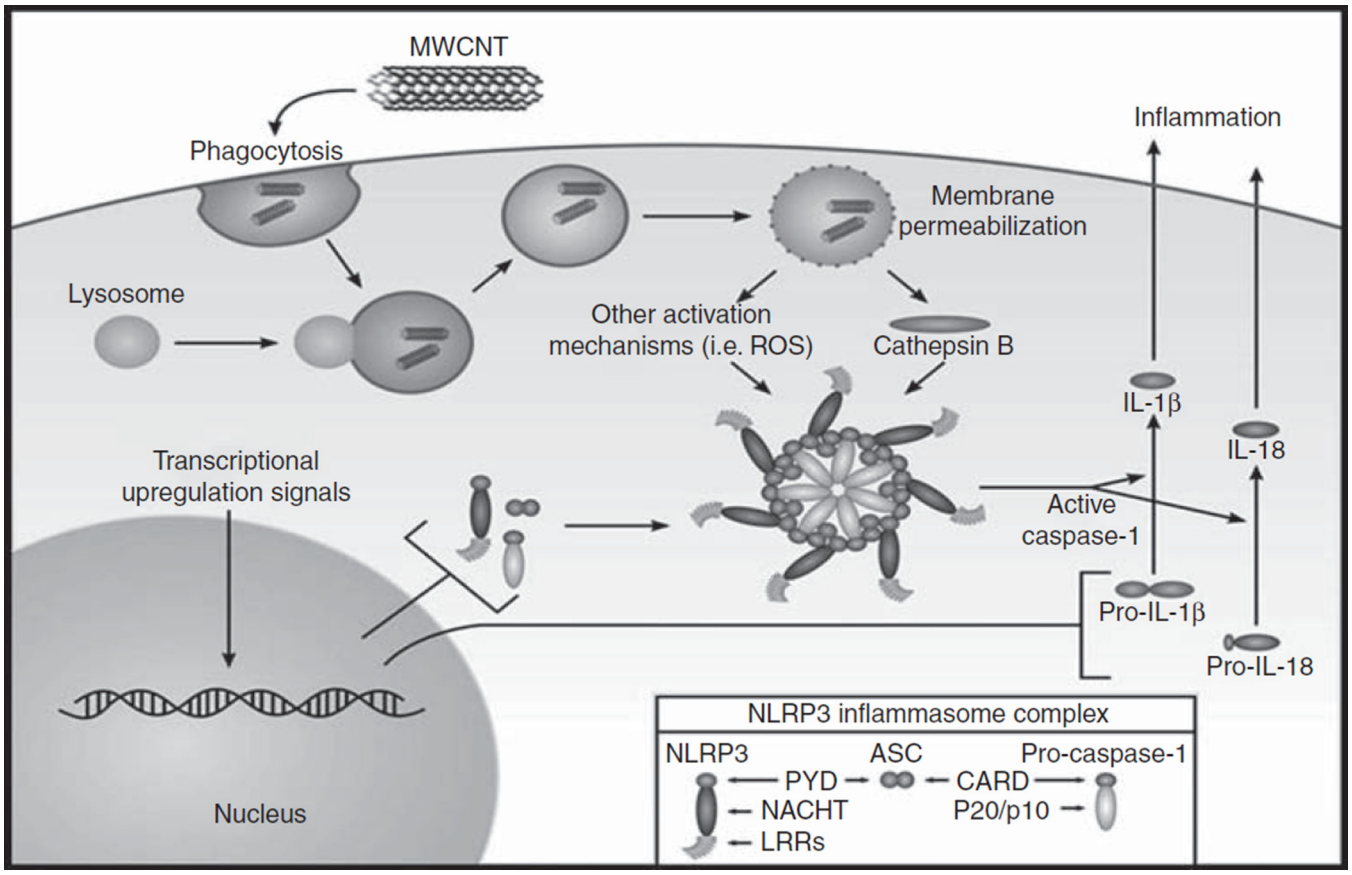

Figure 8.

Schematic of the NLRP3 inflammasome. In this study, the authors propose that the MWCNT being tested will act as danger signals to AMs, initiating an inflammatory cascade mediated through the NLRP3 inflammasome. In this schematic representation, MWCNT disrupt phagolysosomes, releasing cathepsin B and activating the NLRP3 inflammasome. Once activated, the NLRP3 inflammasome cleaves the proinflammatory mediators IL-1β and IL-18, which are subsequently released to initiate the inflammatory cascade.

Author Manuscript Author Manuscript Author Manuscript Author Manuscript

Table I

Summary of histopathological findings.

Post-exposure (days)	Treatment	Total (*n*)	Alveolitis	Fibrosis	Phagocytosed nanoparticles
7	DM	7	0 (*n* = 7)	0 (*n* = 7)	0 (*n* = 7)
	2.5 μg BMWCNT	8	0 (*n* = 8)	0 (*n* = 8)	2 (*n* = 8)*
	2.5 μg FMWCNT	7	0 (*n* = 7)	0 (*n* = 7)	2 (*n* = 7)*
	40 μg BMWCNT	8	0 (*n* = 4)	0 (*n* = 5)	5 (*n* = 8)*
			2 (*n* = 1)	3 (*n* = 2)	
			3 (*n* = 1)	4 (*n* = 1)	
			4 (*n* = 2)		
	40 μg FMWCNT	9	0 (*n* = 8)	0 (*n* = 8)	5 (*n* = 10)*
			2 (*n* = 1)	2 (*n* = 1)	
56	DM	8	0 (*n* = 8)	0 (*n* = 8)	0 (*n* = 8)
	2.5 μg BMWCNT	8	0 (*n* = 8)	0 (*n* = 8)	2 (*n* = 8)*+
	2.5 μg FMWCNT	8	0 (*n* = 8)	0 (*n* = 8)	0 (*n* = 5)*+
					5 (*n* = 3)
	40 μg BMWCNT	8	0 (*n* = 3)*+	0 (*n* = 2)*+	2 (*n* = 2)*+
			2 (*n* = 1)	2 (*n* = 2)	4 (*n* = 3)
			4 (*n* = 4)	4 (*n* = 4)	5 (*n* = 3)
	40 μg FMWCNT	9	0 (*n* = 9)+	0 (*n* = 8)+	0 (*n* = 1)*+
				2 (*n* = 1)	2 (*n* = 6)
					4 (*n* = 1)
					5 (*n* = 1)

BMWCNT, bare multi-walled carbon nanotubes; DM, dispersion medium; FMWCNT, functionalised multi-walled carbon nanotubes.

Values represent histopathology score and inside parentheses the number of animals (n) with that score.

*Significant difference between control and MWCNT group at the same post-exposure time.

+Significant difference between BMWCNT and FMWCNT groups at an equivalent mass dose at the same post-exposure time.